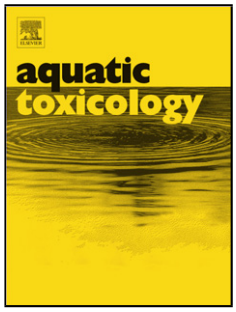

Title: Toxicity assessment of ZnO-decorated Au nanoparticles in the Mediterranean clam *Ruditapes decussatus*

Authors: Badreddine Sellami, Amine Mezni, Abdelhafidh Khazri, Imen Bouzidi, Wiem Saidani, David Sheehan, Hamouda Beyrem

PII: S0166-445X(17)30108-X
DOI: http://dx.doi.org/doi:10.1016/j.aquatox.2017.04.005
Reference: AQTOX 4637

To appear in: *Aquatic Toxicology*

Received date: 26-12-2016
Revised date: 7-4-2017
Accepted date: 9-4-2017

Please cite this article as: Sellami, Badreddine, Mezni, Amine, Khazri, Abdelhafidh, Bouzidi, Imen, Saidani, Wiem, Sheehan, David, Beyrem, Hamouda, Toxicity assessment of ZnO-decorated Au nanoparticles in the Mediterranean clam Ruditapes decussatus.Aquatic Toxicology http://dx.doi.org/10.1016/j.aquatox.2017.04.005

<AT>Toxicity assessment of ZnO-decorated Au nanoparticles in the Mediterranean clam *Ruditapes decussatus*

<AU>Badreddine SELLAMI[a*] ##Email##sellamibadreddine@gmail.com##/Email##, Amine MEZNI[b,c], Abdelhafidh KHAZRI[d], Imen BOUZIDI[d], Wiem SAIDANI[d], David SHEEHAN[e*] ##Email##david.sheehan@kustar.ac.ae##/Email##, Hamouda BEYREM[d]
<AFF>[a]Institut National des Sciences et Technologies de la Mer, Tabarka, Tunisia
<AFF>[b]Unit of Research 99/UR12-30, Department of Chemistry, Faculty of Sciences of Bizerte, 7021 Jarzouna, Tunisia
<AFF>[c]Department of Chemistry, Faculty of Science, Taif University, Taif, Saudi Arabia
<AFF>[d]Laboratoire de Biosurveillance de l'Environnement (LBE), Unité d'Ecotoxicologie et d'Ecologie Côtière (GREEC), Faculté des Sciences de Bizerte, 7021 Zarzouna–Bizerte, Tunisia
<AFF>[e]Environmental Research Institute, University College Cork, Western Gateway Building, Western Road, Cork, Ireland and Khalifa University of Science and Technology, PO Box 127788, Abu Dhabi, United Arab Emirates
<PA>*Correspondences to: (B. Sellami) (D. Sheehan).

<ABS-HEAD>Highlights► We assess the bioavailability and toxicity of Au-ZnO NPs in the clams *Ruditapes decussatus* ► Au-ZnO NPs exposure causes accumulation and deregulation of transitional metals Exposure to Au-ZnO NPs causes an increase in H_2O_2 level, SOD and CAT activities and MDA content ► Au-ZnO NPs exposure disrupts histological structure in both tissues ► Chemical, biochemical and histological analysis could constitute reliable biomarkers for the evaluation of hybrid nanoparticles toxicity.

<ABS-HEAD>Abstract

<ABS-P>The synthesis of hybrid nanomaterials has greatly increased in recent years due to their special physical and chemical properties. However, information regarding the environmental toxicity associated with these chemicals is limited, in particular in the aquatic environment. In the present study, an experiment was performed in which the marine bivalve (*Ruditapes decussatus*) was exposed for 14 days to 2 concentrations of zinc oxide-decorated Au nanoparticles (Au-ZnONPs: Au-ZnONP50 = 50 µg/l; Au-ZnONP100 = 100 µg/l).
<ABS-P>The stability and resistance of Au-ZnONPs in the natural seawater were assessed by combining transmission electron microscopy and dynamic light scattering. Inductively coupled plasma-atomic emission spectroscopy revealed uptake of these nanoparticles within clams and their ability to induce metallic deregulation. The results obtained indicate that Au-ZnONPs induce biochemical and histological alterations within either the digestive gland or gill tissues at high concentration. This was deduced from the significant increase in H_2O_2 level, superoxide dismutase and catalase activities and malondialdehyde content. Furthermore, the toxicity of Au-ZnO nanoparticles was linked with the increase of intracellular iron and calcium levels in both tissues. Histological alterations in gill and digestive gland were more pronounced with Au-ZnONP100 and this is likely related to oxidative mechanisms. Gill and digestive gland are differentially sensitive to Au-ZnONPs if the exposure concentration is higher than 50 µg/L.
<ABS-P>In conclusion, the parameters considered here could constitute reliable biomarkers for evaluation of hybrid nanoparticles toxicity in environmental model organisms. In addition, based on the results obtained, gill and digestive gland of *R. decussatus* could be proposed as models to detect harmful effects of hybrid nanoparticles.

<KWD>Keywords: ZnO-decorated Au nanoparticles; *Ruditapes decussatus*; Biomarkers; oxidative stress.

<H1>1. Introduction

Hybrid nanoparticles (NPs) are promising emerging platforms for developing novel applications in nanoscience. The hybridization can confer better electrocatalytic activity than single component. This offers an effective strategy to enhance the functionality of materials, and paves the way to enhance their electronic, chemical and electrochemical properties (Jasuja and Berry, 2009). Synthesis approaches allow design of a range of NPs for the co-delivery of multiple therapeutic agents or modalities (He et al., 2015).

Metal oxide such as ZnO have low hydrophobicity and their biocompatibility is poor, which has greatly limited their application (Macias-Montero et al., 2012). Recently, ZnO decorated with metal NPs gave high performance in catalysis (Lin et al., 2009) and antibacterial applications (Koga et al., 2009). Meanwhile, metal NPs were introduced on the surface of ZnO to improve the hydrophobicity and biocompatibility of ZnO semiconductor. This revealed a significant decrease in metal nanocluster sintering, dissolution and detachment to prolonged useful lifetimes.

ZnO decorated with Au is considered non toxic, biocompatible and chemically stable and has been used in diverse areas such as multi-modal biological detection (Choi et al., 2008), catalysis (Yu et al., 2010), solar energy conversion (Bang and Kamat, 2009) and opto-electronics applications (Zhang et al., 2010). Despite increasing production and use of hybrid NPs, there is a lack of knowledge about their environmental fate and toxicity. In addition, although the toxicity of the individual nanomaterials is known, the toxicity of the combined component is often not well-understood.

It is increasingly recognized that, after their use cycle, NPs can enter the environment through diverse routes, including solid and liquid waste from domestic sources and industrial activity, accidental spillages, and atmospheric emissions. Several studies have modeled the potential release of NPs into the environment (Canesi et al., 2012; Girardello et al., 2016) and shown that NPs are expected to be found in a range of environmental compartments (i.e., soil, water, air, and landfills). Rigorous identification of environmental hazard and full risk assessments of hybrid NPs are increasingly needed focusing on ecotoxicity of NPs in aquatic systems affecting living organisms. This knowledge should lead to the establishment of an adequate regulatory framework covering hybrid NPs to support more responsible development.

Partly because of their filter-feeding lifestyle, bivalves have previously been widely used as models for investigating toxicity of nanomaterial (Canesi et al., 2012; Buffet et al., 2013; Girardello et al., 2016). *R. decussatus* is an economically important bivalve species, very abundant and well commercialized around the Mediterranean Sea. It is also relatively resistant to a wide variety of pollutants and environmental stressors, making it suitable for marine biomonitoring. These bivalves represent a significant target for NPs in the aquatic environment (Canesi et al., 2012). They were considered as prime candidates for uptake of pollutants from environmental releases (Galloway et al., 2002).

To our knowledge there is no available information on the occurrence of Au-ZnO NPs as pollutants in aquatic ecosystems. However, it is plausible that Au-ZnO NPs may translocate from the seawater to bivalve species, and that secondary adverse effects related to oxidative species may occur to tissue and cellular responses. Oxidative species could be a result of the disruption of the homeostasis of redox-active metals such as iron and calcium. These metals are present in biological systems in a variety of oxidation states and their disruption renders them available as catalysts to produce reactive oxygen species (ROS) such as superoxide radical anion and hydrogen peroxide. ROS-induced biochemical and physiological damage in marine organisms may impair reproduction, inhibit growth, and damage macromolecules such as proteins, DNA and lipids. This triggers on various cellular organelles (Sabatini et al., 2009). ROS are detoxified and controlled by antioxidant defenses which include antioxidant enzymes such superoxide dismutase (SOD) and catalase (CAT). Additionally, Malondialdehyde (MDA) levels increase in NPs-induced toxicity (Ma et al., 2010) and its

predictive importance as a biomarker for oxidative stress has been reported (Xu et al., 2011). Histological tissue changes, resulting from exposure to contaminants, have been also used as marker in biomonitoring studies (Hinton et al., 1992; Papo et al., 2014). Among the different histological markers, the induction of brown cells is considered as indicative of contaminant exposure. Brown cells of bivalve mollusks have been shown to participate in accumulation and detoxification of pollutants (Papo et al., 2014). Based on the fact that *R. decussatus* represents a good model to assess the toxicity of environmental stressors, this study has utilized this bivalve as a model to evaluate the developmental toxicity of Au-ZnO NPs. Furthermore, to better understand the biochemical modifications and tissue damage induced by Au-ZnONPs, the present study determined levels of H_2O_2, MDA, intracellular iron and calcium as well as the activities of SOD and CAT. In addition, the histological structure of gill and digestive gland were also investigated. Our results offer novel insights into the biochemical mechanisms underlying the toxicity caused by Au-ZnONPs on *R. decussatus*.

<H1>2. Materials and methods

<H2>2.1. Synthesis of ZnO-decorated AuNPs

Synthesis of the Au-ZnONPs was achieved in a one-pot chemical process where gold salt $HAuCl_4$ and zinc (II) acetate were mixed together in 1,3-propanediol ($C_3H_8O_2$). The sequential reactions were thermally controlled. The synthesis was carried out in a 100 mL three-neck flask equipped with a condenser, a mechanical stirrer and a thermograph. 0.038 mMol of $HAuCl_4$. $3H_2O$ (Aldrich) were mixed with 0.17 mMol of zinc acetate dehydrate [$(Zn(OAc)_2.2H_2O)$, Aldrich, AR grade] in 50 ml of 1,3-propanediol (ACROS Organics, 98%) with vigorous stirring. First, the mixture was slowly heated to 150°C and kept at that temperature for 10 min, then heated to 160°C and kept at this temperature for 1 h. A violet homogeneous colloidal suspension was obtained. After cooling down to room temperature, the product was separated by centrifugation, washed several times with ethanol/acetone (2:1) and then the powder obtained was re-dispersed in milli-Q water.

<H2>2.2. Structural and morphological characterization

The crystallographic structure of the powder was characterized by X-ray diffraction (XRD) using an INEL diffractometer equipped with a cobalt anticathode (λ= 1.7890Å).

Dynamic light scattering (DLS) of Au-ZnO NPs in the seawater was measured using an Amtec SM 200 Zetasizer operating with a He–Ne laser (632.8 nm).

<H2>2.3. Experimental design and sampling

Clams (*R. decussatus*) were purchased from a site in Bizerte lagoon, Tunisia. Animals were distributed in 3L glass tanks and acclimated for a week on a 12 h light/dark cycle prior to exposure. After the acclimation, three experimental conditions were set up in triplicates of five individuals per tank: Control, Au-ZnONP50 and Au-ZnONP100. Control clams were not exposed to stressor (Au-ZnO NPs). Exposed clams were subjected to daily concentrations of NPs set at 50 µg L^{-1} Au-ZnONP in seawater, corresponding to 35.30 µg of elemental gold and 11.825 µg of Zn elements and 100 µg L^{-1} Au-ZnO NPs in seawater, corresponding to 70.60 µg of elemental gold and 23.65 µg of Zn elements supplied together for a period of 14 days. Au-ZnO NPs concentrations were selected based on environmental relevant concentrations of metal oxide nanoparticles ranged from nanograms to milligrams per liter (Gottschalk et al., 2009; Luo et al., 2011).

After 14 days of exposure, no mortality was observed and all animals were seen to be feeding normally. During the experimental period, salinity, temperature, dissolved oxygen and pH were measured daily with a thermo-salinity meter (LF 196; WTW, Weilheim, Germany), an

oximeter (OXI 330/SET, WTW) and a pH meter (pH 330/SET-1, WTW), respectively. Temperature was maintained at 19 ± 2 °C, oxygen at 6.2 mg/L and the salinity was 32 ‰. Tanks were filled with natural sea water changed every 48 h and the environmental parameters were the same as those used for the acclimation period.

<H2>2.4. Metals content analysis in clams

Clams (n = 5) from each group were dried at 105 °C using a microwave, to constant weight, and then their dry weight is determined gravimetrically with a precision balance. The digestion was performed by adding 3 mL of HNO_3, 3 mL of H_2O_2 and 1 mL of H_2O to each sample. The operating conditions for the microwave digestion system were the following: 720 W for 20 min. After digestion, the extracts were transferred into a graduated polypropylene test tube and diluted with ultrapure water to 50 ml according to Talarico et al. (2014).
Metals content (Au, Zn, Fe, Cu and Mn) was analyzed by inductively coupled plasma-atomic emission spectroscopy (ICP-AES) using reference material of mussel tissue (CRM 278). The detection limits for Au, Zn, Fe, Cu and Mn were in the 0.002–25 mg/L range.
Values reported were corrected for background levels determined in blank sterile filtered seawater.

<H2>2.5. Biochemical analysis

Clams (n = 5) were removed at the end of experiment and fixed in liquid Nitrogen. Gill and digestive gland were then dissected on ice and homogenized by a polytron homogenizer in 10 mM Tris/HCl, pH 7.2, containing 500 mM sucrose, 1 mM EDTA and 1 mM PMSF, supernatants were collected by centrifugation at 20.000 × g (4°C for 30 min).

<H3>2.5.1. Free iron and calcium measurement

Iron levels were determined according to Leardi *et al.* (1998) using a commercially available kit from Biomaghreb, Tunisia. At acidic pH 4.8 all Fe^{3+} released from transferrin was reduced by ascorbic acid into Fe^{2+}, which formed with ferrozine a purple colourful complex measurable at 560 nm. Briefly, gill and digestive gland homogenates were added to reaction mixture containing ascorbic acid (5 g L^{-1}) and ferrozine (40 mM) and incubation performed at 37°C for 10 min.
Ionizable calcium was determined according to Stern and Lewis (1957) using a commercially available kit from Biomaghreb. At basic pH calcium constituted with cresolphtalein a purple colourful complex measurable at 570 nm. Briefly, gill and digestive gland homogenates were added to reaction mixture containing 2-amino-2-methyl 1-propanol buffer (500 mMol/L), cresolphtalein (0.62 mMol/L) and hydroxy-8 quinoleine (69 mMol/L). Incubation was carried out at room temperature for 5 min assuming the complex was stable for 1 hour.

<H3>2.5.2. Antioxidant measurement

SOD activity was assessed by the ability of the enzyme to inhibit auto-oxidation of pyrogallol (Marklund and Marklund, 1974). H_2O_2 levels were measured following the method of Wolff (1994): a volume of 0.1 mL of the supernatant was added to 900 mL of FOX1 reagent (100 mM xylenolorange, 100 mM sorbitol, 250 mM ammonium ferrous sulfate and 25 mM H_2SO_4), vortexed and incubated at room temperature during 30 min. The sample was then centrifuged at 3.000 x *g* for 3 min and the absorbance of the supernatant was read at 560 nm. Catalase (CAT) activity was measured by a decrease in absorbance at 240 nm due to H_2O_2 consumption according to method of Aebi (1974). The reaction volume and reaction time were 1 mL and 1 min, respectively. The reaction solution contained 80 mM phosphate buffer, pH 6.5 and 50 mM H_2O_2 (Ni et al., 1990). Specific SOD and CAT activities are given as nMol/min/ mg protein. Lipid peroxidation was estimated in terms of thiobarbituric acid

reactive species (TBARS), using malondialdehyde (MDA) as standard by the method of Buege and Aust (1978). Sample extract (1 mL) was mixed with 2 mL of the TCA–TBA–HCl reagent (15% TCA, 0.375% TBA and 0.25 NHCl). The contents were boiled for 15 min, cooled and centrifuged at 10.000 g to remove the precipitate. The absorbance was read at 535 nm and the malondialdehyde concentration of the sample was calculated using extinction coefficient of 1.56×10^5 M^{-1}/cm. Lipid peroxidation was expressed as nMol of malondialdehyde (MDA)/mg protein.

<H2>2.6. Histological observations

Routine histology was used to produce tissue sections for histological analyses of digestive gland and gills. In brief, digestive gland and gills were preserved in 4% buffered formalin for 24–72 h, after which the samples were transferred to 50% ethanol. For embedding preparation, digestive gland and gills tissues were dehydrated further through 70%, 96% and absolute ethanol and cleared in xylene, and soaked for 24h in paraffin wax (Paraplast, Fluka, Germany) using Leica-TP 1020 (Leica, Germany) processor. Tissues were placed in blocks filed with liquid paraffin at 60°C. After cooling, sections were cut at 2 µm using a microtome Leica RM 2125 RT (Leica, Germany) and dewaxed overnight in an oven at 60 °C. Dried sections were stained with haematoxylin and eosin stains (Sigma-Aldrich). After staining, sections were dehydrated in increasing concentrations of ethanol (70–100%), cleared in xylene, and mounted in Biomount DPX (Sigma-Aldrich).Tissue sections were examined microscopically using Leica DM 2500 microscope (Leica, Germany). Microphotographs were taken using digital camera (Moticam 352) connected to microscope.

<H2>2.7. Statistical analyses

Statistical analysis was carried out using a statistical package (STATISTICA 8.0). Results of enzymatic activities, intracellular free iron, calcium and metal content were reported as mean ± standard deviation. The variation of each parameter among concentration was tested by one-way ANOVA ($p < 0.05$). Previously we tested the pre-requisites for analysis of variance (normality and homogeneity of variances).When significant differences were found, Tukey's test was applied to determine which values differed significantly.

<H1>3. Results

<H2>3.1. Characterization of ZnO-decorated Au nanoparticles

The XRD patterns of pure ZnO NPs and Au-ZnO NPs are shown in Figure 1. All the diffraction peaks of ZnO can be indexed to hexagonal wurtzite ZnO with the strong (100), (002), (101) characteristic peaks (JCPDS No. 36-1451). The XRD pattern of the Au-ZnO NPs is very similar to that of pure ZnO NPs, indicating that the formation of Au in the reaction process has no influence on the crystal structure of the ZnO. Besides the diffraction peaks of ZnO NPs, three additional diffraction peaks were present at θ= 38.33, 44.21 and 64.79° and were assigned, respectively, to the diffraction lines of the (111), (200) and (220) planes of FCC gold (JCPDS No. 65-2870). The XRD results indicated that the synthesized nanoparticles have good crystallinity.

As shown by the transmission electron microscopy (TEM), presented in Figure 2-a, the as synthesized nanoparticles consist mainly of faceted quasi-spherical gold cores (around 10-40 nm) surrounded by closely packed zinc oxide NPs (3-5 nm) forming a decoration. Figure 2-b, shows the influence of Au-ZnO NPs after exposure to the clams' shell. As shown and compared to the TEM images of pure Au-ZnO nanoparticles (Figure 1-a), the size of gold and ZnO particles were altered. Indeed, the size of pure Au-ZnO NPs as shown in Figure 1-a, is in the range of 30 nm however is about 85 nm (Fig.2-b) in seawater. The EDX spectrum presented in Figure 2-c, indicates that the NPs are of a high purity, since only Au, O and Zn elements are detected. The presence of Cu is due to the copper grid used for the TEM/EDX

experiments, the Fe and Co elements are due to the pole components of the microscope. Figure 2-d presents selected area electron diffraction (SAED) pattern obtained with the electron beam incidence perpendicular to the face of a single Au-ZnO NPs. The linear symmetrical spots of the SAED pattern shows well-defined ZnO crystal planes thus corroborating the crystalline structure of the formed Au-ZnO NPs.

Figure 3 demonstrates a monomodal scattered intensity distribution with a major maximum at about 82 nm. According to the DLS data (Fig. 3), the Z-average particle diameter is d_{av} = 82 ± 1 nm and the average relative half width of the distribution is σ = 10 ± 1 nm. As can be seen, the position of the major peak of the scattered intensity distribution (d ≈ 82 nm,) exceeds the size dispersion obtained from TEM images (Au-ZnO NPs with an average size around 50 and 70 nm). From DLS we obtain the hydrodynamic diameter of the particle, defined as a sphere with the same translational diffusion coefficient as the particle being measured (assuming a hydration layer surrounding the particle or molecule). Hence we can attribute this small different between the size of Au-ZnO NPs obtained by DLS and TEM to the hydrodynamic diameter measured and added by DLS. As a result, it is concluded according to DLS and TEM data that Au-ZnO NPs are stable in seawater and no agglomeration or aggregation was observed.

Particle size can be determined by measuring the random changes in the intensity of light scattered from a suspension or solution this is the main principle of DLS technique. Indeed, DLS measures Brownian motion and relates this to the size of the particles. Brownian motion is the random movement of particles due to the bombardment by the solvent molecules that surround them. Normally DLS is concerned with measurement of particles suspended within a liquid. The larger the particle, the slower the Brownian motion will be. Smaller particles are ``kicked'' further by the solvent molecules and move more rapidly. The size of a particle is calculated from the translational diffusion coefficient by using the Stokes-Einstein equation;

$$d(H)= kT/ 3\pi\eta D$$

Where: d(H) = hydrodynamic diameter, D = translational diffusion coefficient, k = Boltzmann's constant, T = absolute temperature and η = viscosity

Note that the diameter that is measured in DLS is a value that refers to how a particle diffuses within a fluid so it is referred to as a hydrodynamic diameter. The diameter that is obtained by this technique is the diameter of a sphere that has the same translational diffusion coefficient as the particle. The translational diffusion coefficient will depend not only on the size of the particle ``core'', but also on any surface structure, as well as the concentration and type of ions in the medium.

<H2>3.2. Metals concentration in R. decussatus

Table 1 illustrates the metal (Au, Zn, Fe, Cu and Mn) concentration in the whole soft tissue of clams after exposure to 50 and 100 µg/L of Au-ZnO NPs for 14 days. Metals concentration statistically significantly increased in concentration-dependent pattern compared to controls. The higher increase was shown by the group of clams exposed to Au-ZnONP100 compared to the clams exposed Au-ZnONP50 and control groups. Au was not detected in control group and increased significantly in concentration dependant pattern after exposure to Au-ZnONPs. Zn increased specifically in treated clams with Au-ZnONP100 by about and 76% compared to

control clams. Additionally, Fe and Cu were also statistically significantly increased in treated clams with Au-ZnONP100 compared to control clams by about 35 and 29%, respectively.

<H2>3.3. Measurement of intracellular calcium and iron concentrations

Free iron and ionizable calcium levels were measured in gill and digestive gland in response to Au-ZnO NPs (Fig. 4a,b). No significant difference was observed in both organs after 14 days of exposure to Au-ZnONP50 compared to controls. In contrast, free iron and calcium levels were increased respectively by 31 and 33% in gills and by 45 and 53% in digestive gland of clams exposed to Au-ZnONP100 compared to control clams.

<H2>3.4. Oxidative response and lipid peroxidation estimation in clams exposed to Au-ZnO nanoparticles

Figure 4c,d,e,f illustrates changes in SOD activity, H_2O_2 production, CAT activity and TBARS content in gill and digestive gland of control and treated clams with Au-ZnONPs. No statistically significant changes in SOD activity were detected in gills and digestive gland tissues after exposure to 50 µg/L of Au-ZnONPs. However, exposure to 100 µg/L of Au-ZnONPs increased SOD activity by 34 and 39% in gill and digestive gland, respectively. In addition, a significant increase in H_2O_2 production in gill and digestive gland was observed when clams were exposed to 100 µg/L of Au-ZnONPs. The highest increase in H_2O_2 production was observed on the digestive gland at a concentration of 100 µg/L with 30% increase compared to its respective control. CAT activity increased also by 18 and 23%, respectively, in gill and digestive gland of clams exposed to Au-ZnONP100. No significant difference was observed in CAT activity after exposure to Au-ZnONP50 in both tissues.

Relative to controls and judged by TBARS content, no statistically significant changes in lipid peroxidation were detected in gill and digestive gland tissues of clams after 14 days of exposure to Au-ZnONP50 (Fig. 4f). However, statistically significant differences in levels of lipid peroxidation were observed at the higher exposure concentrations of Au-ZnONP (100 µg/L). MDA content increased in the digestive gland from 4.17 to 8.27 nmol/mg proteins and from to 3.61 to 6.23 nmol/mg proteins in gills after exposure to Au-ZnONP100.

<H2>3.5. Histological effects of Au-ZnO nanoparticles

Effects of Au-ZnO NPs treatment over the entire experiment, after fourteen days of exposure upon histological features of experimental clams are shown in Figure 5 and 6.

Histological analyses in digestive gland of control animals after 14 days (Fig. 5B) demonstrated normal digestive tubule structure comparable with the control group prior to exposure (Fig. 5A). After 14 days of exposure to Au-ZnONP50 no modifications were observed compared to control (Fig. 5C). In contrast, exposure to Au-ZnONP100 nanoparticles induced histological changes such as atrophy of digestive tubules, increase of hemocytic infiltration, intensity of cell vacuolation and number of brown cells (Fig. 5D).

Histological analyses in gill of control group after 14 days of experiment (Fig. 6B) demonstrated normal arch structure and branchial lamellae having the same structure as in the

control group prior to exposure (Fig. 6A). After 14 days of exposure to Au-ZnONPs, histological changes such as increase of intensity of cell vacuolation and number of brown cells were observed. These changes were dependant to NPs concentration with more pronounced effects detected after exposure to Au-ZnONP100 (Fig. 6C,D).

<H1>4. Discussion

The aquatic environment and wildlife are constantly exposed to several kinds of NPs. Hybrid NPs have aroused great concern in recent years. However, there remains the question whether their environmental toxicity. In this study, we used the clam *Ruditapes decussatus* to assess the bioavailability of Au-ZnO NPs and their effects.

<H2>4.1. Bioavailability of Au-ZnO NPs in R. decussatus and metals variation

Data on Au-ZnO NPs characterization in the natural seawater at pH 7.6 used in the present study, did not show NPs aggregation indicating NPs stability. Thus, depending on size and morphology in the seawater media, Au-ZnO NPs can be considered as ``nanoparticles resistant to salt'' and can be proposed indeed as a model contaminant for ecotoxicology studies (García-Negrete *et al*., 2013). This result support the data obtained by García-Negrete et al. (2013) and Teles et al. (2016) in terms of behaviour of Au-citrate NPs at low concentration in the seawater and Au NPs coated polyvinylpyrrolidone in salt water where NPs maintained their characteristics during the experimentation. According to these findings, we can suggest that Au-ZnO NP may remain available in the water column for a significant time-period. Marine bivalves have an ability to concentrate dissolved or suspended contaminants that may be present in low concentrations in the water media. Metal concentration analysis using ICP-AES in clams showed that exposure to Au-ZnONP100 resulted in a significant increase of Fe, Cu and especially Au and Zn concentration. These observations give support for suggesting that the Au-ZnONP100 induce a dysregulation of metal concentration in the tissue and confirm the bioavailability of these NPs to the clam. Our results are in agreement with a previous study reporting accumulation of combined NPs in bivalves (Tedesco et al., 2010). Au and Zn concentration increased after exposure to Au-ZnO NPs in concentration dependant manner. Comparable results were announced by Marisa et al. (2015) in the clam *Ruditapes philippinarum* exposed to titanium dioxide (TiO_2) nanoparticles where accumulation of the Ti increases with the concentration of TiO_2 NPs. These authors correlated an increase in metal elements to bio-accumulation of these xenobiotics. Trevisan et al. (2014) showed that a concentration of 4 mg/l of ZnO is suitable to induce an accumulation of NPs in the oyster *Crassostrea gigas.* Moreover, the contamination of this same species by CuO NPs revealed accumulation of these particles in a concentration-dependent pattern. A significant bio-accumulation of CuO NPs was confirmed in *Mytilus edulis* exposed to different concentrations of CuO NPs (Hu *et al.*, 2014).

Metals, such as Zn, Fe, Cu and Mn are essential for aquatic organisms and considered as transitional metals due to their great participation in metabolic reactions, serving as cofactors for several enzymes (Saad, 2003; Mathie et al., 2006). In the present study, a modest increase of iron and copper as revealed by ICP-AES analysis in the clam tissues may possibly relate to metabolic process as a defensive response to Au-ZnO NPs exposure. Fe and Cu are implicated in biochemical processes for detoxification of free radicals generated following the contamination (Vale *et al.,* 2016). It's also known that Zn and Cu are correlated with each other and regulated by Metallothioneins (Santon et al., 2008). Thus, increase of Cu is related to the amount of Zn highly increased after exposure to Au-ZnO nanoparticles. Our results are in agreement with previous study that showed an increase in the concentrations of iron,

copper and zinc, correlated with an increase in ZnO NPs concentration in the fish *D. rerio* (Vale *et al.,* 2016).

<H2>4.2. Effect of contamination on biochemical and histological status

Integration of biochemical and chemical analysis is widely recommended in environmental toxicity studies as it permits the integrated correlation of pollutants exposure to biological effects on sentinel species (de los Ríos et al., 2013). In the present study, exposure of *R. decussatus* to Au-ZnO NPs suspensions, at nominal concentrations of 50 and 100 µg L^{-1} for 14 days, significantly affected different molecular and histological parameters of the gill and digestive gland.

These represent the first data on the *in vivo* effects of Au-ZnO NPs on oxidative status and on the histological effects of Au-ZnO NPs in marine invertebrates. The obtained results indicate that, at high concentration and shorter time of exposure, Au-ZnO NPs induce deregulation of biochemical parameters in clams. In fact, an increase in free iron (Fe) and ionizable calcium (Ca) concentration was detected after exposure to 100 µg/l of Au-ZnO NPs. This result was reported in *Mytilus galloprovincialis* exposed to silver nanoparticles (Gagné *et al.,* 2016). These authors showed that the level of metal elements increases after contamination and that increase in Ca concentration correlates with the increase in Zn concentration in the organism.

H_2O_2 is produced in specific cellular compartments and is a potent second messenger in regulating various important biological processes. In the present study, H_2O_2 increase in gill and digestive gland after exposure to Au-ZnONP100 suggesting that both organs are sensitive to Au-ZnO NPs at high concentrations. Similarly, Trevisan et al. (2014) showed that gill and digestive gland are sensitive to ZnONPs at high concentration, leading to mitochondria membrane disruption. Iron catalyzes formation of ROS through the Haber–Weiss and Fenton reactions (Halliwell, 2006). Therefore, an increase of free iron level in gill and digestive gland of *R. decussatus* and its deregulation participate in an increase of H_2O_2.

At 50 µg/L of Au-ZnO NPs no modification was detected in gill and digestive gland. This result is probably due to the interactive response of Zn and ROS. In fact, Zn is an essential element and well-known to act as an antioxidant metal at low concentrations in cells (Gagné et al., 2016). Furthermore, low oxidation states can catalyze decomposition of H_2O_2 *via* the Fenton reaction, which yields hydroxyl radicals (Lloyd et al., 1997). The protective effects of Zn against H_2O_2 involved glucose-6-phosphate dehydrogenase and glutathione S-transferase. The addition of a membrane permeable zinc chelator blocked their expression in support of its antioxidative properties.

Increased of H_2O_2 after exposure to Au-ZnONP100 could be a result of SOD activation. SOD scavenges superoxide radical anions by either the removal or addition of an electron, so resulting in H_2O_2. In this study, SOD activity in the gill and digestive gland was measured to further confirm the obtained result for H_2O_2. Our data showed that SOD activity increased significantly after exposure to Au-ZnONP100 but no effect was observed at Au-ZnONP50. This result suggests that clams may be vulnerable to oxidative stress if the exposure concentration is higher than 50 µg/L.

CAT is considered as a second line of defense against ROS with its high affinity for H_2O_2 (Orbea et al., 2000). This enzyme converts H_2O_2 to oxygen and water in order to minimize the oxidative stress induced by ROS (Pi et al., 2010). CAT and SOD work together to eliminate ROS in order to reduce the oxidative stress (Uner et al., 2001). In the present study, CAT activity increased significantly in gill and digestive gland of clams after 14 days of exposure to Au-ZnONP100. These data are in line with recent observations that nanoparticles increased SOD and CAT activities at high concentrations and related this modification to oxidative stress induced by ROS (Canesi et al., 2010; Girardello et al., 2016).

ROS overproduction overwhelmed the antioxidant system efficiency of cells to maintain redox balance (De Marchi et al., 2017). The excess of ROS caused by NPs lead to lysosomal membrane destabilization, impairment of phago-lysosomal system, proteins and DNA damages (Chen et al., 2006; Gomes et al., 2012; Barmo et al., 2013; Ruiz et al., 2015)
A redox imbalance in clam tissues can lead also to lipid peroxidation and histological modifications through a free radical mechanism. Our data showed that TBARS levels, marker of lipid peroxidation, increased significantly in gill and digestive gland after exposure to Au-ZnONP100. This result demonstrates that a high concentration of Au-ZnO NPs induce lipid peroxidation potentially causing changes in membrane fluidity. Similar results were observed after exposure to NPs suggesting that nanomaterial is capable of crossing cell membranes, leading to cell damage (Li et al., 2010). In addition, NPs toxicity is often associated to their internalization within cells, entry and storage in lysosomes, endoplasmic reticulum or golgi apparatus triggering oxidative damage and lipid peroxidation (Moore, 2006). Histological analysis revealed pronounced effect of Au-ZnONP100 in gill and digestive gland structure as a result of oxidative mechanism and lipid accumulation. Indeed, alterations in gills were associated with increase of number of brown cells, suggesting oxidative stress. It has been suggested that once pollutants enter the organisms, one of the inner defense mechanisms of the molluscs include the participation of hemocytes and brown cells (Papo et al., 2014).These cells contain lipofuscin-like pigments constituted of non-degradable material, resulting mainly from accumulation of oxidized proteins and lipids (Lassudrie et al., 2014). In bivalves, haemocytic infiltration has been linked to histological changes due to numerous factors including contaminants (Sheir and Handy, 2010; Costa et al., 2013), suggesting that in our experimental conditions the increasing in brown cell number is due to Au-ZnO NPs exposure. Several authors found that molluscs from clean sites exhibited a reduced number of brown cells in comparison with those from polluted sites (Zaroogian and Yevich, 1993; Costa et al., 2013).
Alterations observed histologically in gills and digestive gland of clams have been reported after exposure to heavy metals or complex mixtures of environmental pollutants (Javed and Usmani, 2013; Barišić et al., 2015). Our results suggest also that clams may be vulnerable to several alterations of tissues if the exposure concentration is higher than 50 µg/L because no modifications were observed with Au-ZnONP50 compared to controls.
<H1>5. Conclusion

Results reported here show that, Au-ZnO NPs are available in the seawater column due to their stability. ICP-AES analysis showed that Au-ZnO NPs accumulated significantly after only 14 days of exposure leading to metallic deregulation. Induction of oxidative stress parameters (SOD, H_2O_2, CAT and MDA) and histological alterations were also detected in a concentration-dependent pattern. As a consequence, exposure to high concentration of Au-ZnO NPs causes oxidative stress, an increase in lipid peroxidation and damage to gill and digestive gland tissue structure. Monitoring of hybrid NPs is required since toxic effects can occur if they appear at high concentrations in the aquatic ecosystems, the present study provides valuable information regarding the potential risk to the environment and living organisms. Thus, further investigations focusing on long-term effects of hybrid NPs at low concentrations and the possibility of their chemical modification to reduce such effects are warranted.

Acknowledgments

This work was supported by grants from the National Institute of Marine Sciences and Technologies, Tabarka, The Ministry of Higher Education of Carthage (Tunisia), Laboratory of Environment Biomonitoring, Unit of research 99/UR12-30, Department of Chemistry,

Faculty of Sciences of Bizerte 7021 Jarzouna (Tunisia) and Environmental Research Institute and School of Biochemistry and Cell Biology, University College Cork, Western Gateway Building, Western Road, Cork, Ireland.

<REF>References

<BIBL>

Aebi, H.,;1; 1974. Catalase In: Bergmeyer, H.U.(Ed.), Methods of Enzymatic Analysis. <PN>Academic Press</PN>, <PL>London</PL>, pp. 671–684.

Bang, J., Kamat, P.V.,;1; 2009. Quantum Dot Sensitized Solar Cells. A Tale of Two Semiconductor Nanocrystals: CdSe and CdTe. ACS Nano 3, 1467-1476.

Barišić, J., Dragun, Z., Ramani, S., Marijić, V.F., Krasnići, N., Čož-Rakovac, R., Kostov, V., Rebok, K., Jordanova, M.,;1; 2015. Evaluation of histopathological alterations in the gills of Vardar chub (*Squalius vardarensis Karaman*) as an indicator of river pollution. Ecotoxicology and Environmental Safety 118, 158–166.

Barmo, C., Ciacci, C., Canonico, B., Fabbri, R., Cortese, K., Balbi, T., Marcomini, A., Pojana, G., Gallo, G., Canesi, L.,;1; 2013. *In vivo* effects of n-TiO2 on digestive gland and immune function of the marine bivalve *Mytilus galloprovincialis*. Aquat. Toxicol. 132–133, 9–18.

Buege, J.A., Aust, S.D.,;1; 1978. Microsomal lipid peroxidation. MethodsEnzymol. 52, 302–310.

Buffet, P.E., Pan, J.F., Poirier, L., Amiard-Triquet, C., Amiard, J.C., Gaudin, P., Risso- de Faverney, C., Guibbolini, M., Gilliland, D., Valsami-Jones, E., Mouneyrac, C.,;1; 2013. Biochemical and behavioural responses of the endobenthic bivalve *Scrobicularia plana* to silver nanoparticles in seawater and microalgal food. Ecotoxicol. Environ. Saf. 89,117–124.

Canesi, L., Ciacci, C., Fabbri, R., Marcomini, A., Pojana, G., Gallo, G.,;1; 2012. Bivalve molluscs as a unique target group for nanoparticletoxicity. Mar. Environ. Res. 76, 16–21.

Canesi, L., Fabbri, R., Gallo, G., Vallotto, D., Marcomini, A., Pojan, G.,;1; 2010. Biomarkers in *Mytilus galloprovincialis* exposed to suspensions of selected nanoparticles (Nano carbon black, C60 fullerene, Nano-TiO_2, Nano-SiO_2) Aquatic Toxicology 100, 168–177.

Chen, Z., Meng, H., Xing, G., Chen, C., Zhao, Y., Jia, G., Wang, T., Yuan, H., Ye, C., Zhao, F., Chai, Z., Zhu, C., Fang, X., Ma, B., Wan, L.,;1; 2006. Acute toxicological effects of copper nanoparticles in vivo. Toxicol. Lett. 163, 109-120

Choi, S., Na, H.B., Park, Y., K, An.,;1; Kwon, S.G., Jang, Y., Park, M., Moon, J., Son, J.S., Song, I.C., Moon, W.K., Hyeon T., 2008. Simple and Generalized Synthesis of Oxide−Metal Heterostructured Nanoparticles and their Applications in Multimodal Biomedical Probes J. Am. Chem. Soc. 130, 15573-15580.

Costa, P.M., Carreira, S, Costa, M.H., Caeiro, S.;1; 2013. Development of histopathological indices in a commercial marine bivalve (*Ruditapes decussatus*) to determine environmental quality. Aquat. Toxicol. 126, 442-454.

de los Ríos, A., Pérez,;1; L., Ortiz-Zarragoitia, M., Serrano, T., Barbero, M.C., Echavarri-Erasun, B., Juanes, J.A., Orbea, A., Cajaraville, M.P., 2013. Assessing the effects of treated and untreated urban discharges to estuarine and coastal waters applying selected biomarkers on caged mussels. Marine Pollution Bulletin 77 (2013) 251–265.

De Marchi, L., Neto, V., Pretti, C., Figueira, E., Chiellini, F., Soares, A.M.V.M., Freitas, R.,;1; 2017. The impacts of emergent pollutants on *Ruditapes philippinarum*: biochemical

responses to carbon nanoparticles exposure. Accepted Manuscript.
<DOI> http://dx.doi.org/doi:10.1016/j.aquatox.2017.03.010</DOI>
Gagné, F., Turcotte, P., Pilote, M., Auclair, J., André, C., Gagnon, C.;1; 2016. Elemental profiles of freshwater mussels treated with silver nanoparticles: A metallomic approach. Compare. Biochem. Physio. Part C. 188, 17-23
Galloway, T.S., Sanger, R.C., Smith, K.L., Fillmann, G., Readman, J.W., Ford, T.E., et al.;1; 2002. Rapid assessment of marine pollution using multiple biomarkers and chemical immunoassays. Environ Sci Technol. 36, 2219–26.
García-Negrete, C.A., Blasco, J., Volland, M., Rojas, T.C., Hampel, M., Lapresta-Fernández, A., Jiménez de Haro, M.C., Sotoc, M., Fernández, A.,;1; 2013. Behaviour of Au-citrate nanoparticles in seawater and accumulation in bivalves at environmentally relevant concentrations Environmental Pollution 174, 134-141.
Girardello, F., Leite, C.C., Branco, C.S., Roesch-Ely, M., Fernandes, A.N., Salvador, M., Henriques, J.AP.,;1; 2016. Antioxidant defences and haemocyte internalization in Limnoperna fortunei exposed to TiO2 nanoparticles Aquatic Toxicology 176, 190–196.
Gomes, T., G. Pereira, C., Cardoso, C., Pinheiro, J.P., Cancio, I., Bebianno, M.J.,;1; 2012. Accumulation and toxicity of copper oxide nanoparticles in the digestive gland of *Mytilus galloprovincialis*. Aquat. Toxicol. 118–119, 72–79.
Gottschalk, F., Sonderer, T., Scholz, R.W., Nowack, B.,;1; 2009. Modeled environmental concentrations of engineered nanomaterials (TiO_2, ZnO, Ag, CNT, fullerenes) for different regions. Environ. Sci. Technol. 43, 9216–9222.
Halliwell B.,;1; 2006. Oxidative stress and neurodegeneration: where are we now? J. Neurochem. 97, 1634–1658.
He, C., Lu, J. Lin, W.,;1; 2015. Hybrid nanoparticles for combination therapy of cancer. Journal of Controlled Release 219, 224–236.
Hinton, D.E., Baumann, P.C., Gardner, G.R., Hawkins, W.E., Hendricks, J.D., Murchelano, R.A., et al.;1; 1992. Histopathologic biomarkers. In: Huggett, R.J, Kimerle, R.A., Mehrle, P.M., Bergman H.L., editors. Biomarkers. <PL>Boca Raton, Ann Arbor, London, Tokyo: </PL> <PN>Lewis Publishers</PN>; 155-209.
Hu, W., Culloty, S., Darmody, G., Lynch, S., Davenport, J., Ramirez-Garcia, S.,n Dawson, K.A., Lynch, I., Blasco, J., Sheehan, D.,;1; 2014. Toxicity of copper oxide nanoparticles in the blue mussel, *Mytilus edulis*: A redox proteomic investigation. Chemosphere 108: 289–299.
Jasuja, K., Berry, V.,;1; 2009. Implantation and Growth of Dendritic Gold Nanostructures on Graphene Derivatives: Electrical Property Tailoring and Raman Enhancement. ACS Nano 3, 2358–2366.
Javed, M., Usmani, N.,;1; 2013. Assessment of heavy metal (Cu, Ni, Fe, Co, Mn, Cr, Zn) pollution in effluent dominated rivulet water and their effect on glycogen metabolism and histology of Mastacembelus armatus. SpringerPlus 2, 390.
Koga, H., Kitaoka, T., Wariishi, H.,;1; 2009. On-paper synthesis of Au nanocatalysts from Au(III) complex ions for low-temperature CO oxidation. J. Mater. Chem. 19 2135–2140
Lassudrie, M., Soudant, P., Richard, G., Henry, N., Medhioub, W., da Silva, P.M., Donval, A., Bunel, M., Le Goïc, N., Lambert, C., de Montaudouin, X., Fabioux, C., Hégaret, H.,;1; 2014. physiological responses of manila clams *Venerupis* (= *Ruditapes*) *philippinarum* with varying parasite *perkinsus olseni* burden to toxic algal *alexandrium ostenfeldii* exposure. Aquatic Toxicol 154, 27-38.

Leardi, A., Caraglia, M., Selleri, C., Pepe, S., Pizzi, C., Notaro, R.,;1; 1998. Desferioxamine increases iron depletion and apoptosis induced by ara-C of human myeloid leukaemic cells. Br J Haematol 102:746–752.

Li, J., Zhu, Y., Li W., Zhang, X., Peng, Y., Huang, Q.,;1; 2010. Nanodiamonds as intracellular transporters of chemotherapeutic drug, Biomaterials 31, 8410–8418.

Lin, D., Wu, H., Zhang, R., Pan, W.,;1; 2009. Enhanced Photocatalysis of Electrospun Ag−ZnO Heterostructured Nanofibers. Chem. Mater. 21, 3479–3484.

Lloyd, R.V., Hanna, P.M., Mason, R.P.,;1; 1997. The origin of the hydroxyl radical oxygen in the Fenton reaction. Free Radic Biol Med. 22, 885–888.

Luo, Z., Wang, Z., Li, Q., Pan, Q., Yan, C., Liu, F.,;1; 2011. Spatial distribution, electron microscopy analysis of titanium and its correlation to heavy metals: occurrence and sources of titanium nanomaterials in surface sediments from Xiam en Bay, China. J. Environ. Monit. 13,1046–1052.

Ma, L.L., Liu, J., Li, N., Wang, J., Duan, Y.M., Yan, J.Y., Liu, H.T., Wang, H., Hong, F.S.,;1; 2010. Oxidative stress in the brain of mice caused by translocated nanoparticulate TiO_2 delivered to the abdominal cavity. Biomaterials 31, 99–105

Macias-Montero, M., Borras, A., Saghi, Z. Romero-Gomez, P., Sanchez-Valencia, J.R., Gonzalez, J.C., Barranco, A., Midgley, P., Cotrino, J., Gonzalez-Elipe, A.R.,;1; Superhydrophobic supported Ag-NPs@ZnO-nanorods with photoactivity in the visible range. Journal of Materials Chemistry 22, 1341-1346

Marisa, I., Marin, M.G., Caicci, F.G., Franceschinis, E.,;1; Martucci, A., Matozzo, V., 2015. In vitro exposure of haemocytes of the clam *Ruditapes philippinarum* to titanium dioxide (TiO_2) nanoparticles: Nanoparticle characterisation, effects on phagocytic activity and internalisation of nanoparticles into haemocytes. Mar. Environ. Res. 103: 11-17

Marklund, S., Marklund, G.,;1; 1974. Involvement of the superoxide anion radical in the autoxidation of pyrogallol and a convenient assay for superoxide dismutase. Eur. J. Biochem. 47, 469–474.

Moore, M.N.,;1; 2006. Do nanoparticles present ecotoxicological risks for the health of the aquatic environment? Environ. Int. 32, 967–976.

Ni, W., Trelease, R.N., Eising, R.,;1; 1990. Two temporally synthesized charge subunits interact to form the five isoformes of cottonseed (Gossypium hirsutum) catalase. Biochemistry 269, 233–238.

Orbea, A., Fahimi, H.D., Cajaraville, M.P.,;1; 2000. Inmunolocalization of fouranti- oxidant enzymes in digestive glands of mollusks and crustaceans and fish liver. Histochem. Cell Biol. 114,393–404.

Papo, M.B., Bertotto, D., Pascoli, F., Locatello, L., Vascellari, M., Poltronieri, C., Quaglio, F., Rada, G.;1; 2014. Induction of brown cells in *Venerupis philippinarum* exposed to benzo(a)pyrene. Fish & Shellfish Immunology 40, 233-238.

Pi, J., Zhang, Q., Fu, J.G., Woods, C.G., Hou,Y., Corkey, B.E., Collins, S., Andersen, M.E.,;1; 2010. ROS signaling, oxidative stress and Nrf2 in pancreatic beta-cell function. Toxicol. Appl. Pharmacol. 244, 77–83.

Ruiz, P., Katsumiti, A., Nieto, J.A., Bori, J., Jimeno-Romero, A., Reip, P., Arostegui, I., Orbea, A., Cajaraville, M P.,;1; 2015. Short-term effects on antioxidant enzymes and long-term genotoxic and carcinogenic potential of CuO nanoparticles compared to bulk CuO and ionic copper in mussels *Mytilus galloprovincialis*. Mar. Environ. Res. 111, 107-120.

Saad, M.A.H.,;1; 2003. Impact of Diffuse Pollution on The Socio-Economic Development Opportunities in The Coastal Nile Delta Lakes. Diffuse Pollution Conference Dublin, ECSA 5, Management, p. 83.

Sabatini, S.E., Juarez, A.B., Eppis, M.R., Bianchi, L., Luquet, C.M., Molina, M.C.,;1; 2009. Oxidative stress and antioxidant defenses in two green microalgae exposed to copper. Ecotoxicology and Environment Safety 72, 1200–1206.

Santon, A., Formagari, A., Irato, P.,;1; 2008. The influence of metallothionein on exposure to metals: an in vitro study on cellular models. Toxicol. in Vitro 22, 980–987.

Sheir, S.K., Handy, R.D.,;1; 2010. Tissue injury and cellular immune responses to cadmium chloride exposure in the common mussel *Mytilus edulis*: modulation by lipopolysaccharide. Arch. Environ. Contam. Toxicol. 59, 602-613.

Stern, J., Lewis, W.H.,;1; 1957. the colorimetric estimation of calcium in serum with ocresolphthalein complexone. Clin. Chim. Acta 2:576–580.

Talarico, F., Brandmayr, P., Giulianini, P.G., Ietto, F., Naccarato, A., Perrotta, E., Tagarelli, A., Giglio, A.,;1; 2014. Effects of metal pollution on survival and physiological responses in Carabus (Chaetocarabus) lefebvrei (Coleoptera, Carabidae). Eur J Soil Biol 61:80–89.

Tedesco, S., Doyle, H., Blasco, J., Redmond, G., Sheehan, D.,;1; 2010. Exposure of the blue mussel, *Mytilus edulis*, to gold nanoparticles and the pro-oxidant menadione. Comparative Biochemistry and Physiology C e Toxicology & Pharmacology 151, 167-174.

Teles, M., Fierro-Castro, C., Na-Phatthalung, P., Tvarijonaviciute, A., Trindade, T., Soaresd, A.M.V.M., Torta, L., Oliveira, M.,;1; 2016. Assessment of gold nanoparticle effects in a marine teleost (*Sparus aurata*) using molecular and biochemical biomarkers Aquatic Toxicology 177, 125–135.

Trevisan, R., Delapedra, G., Mello, D.F., Arl, M., Schmidt, E.C., Meder, F., Monopoli, M., Cargnin-Ferreira, E., Bouzon, Z.L., Fisher, A.S., Sheehan, D., Dafre, A.L.,;1; 2014. Gills are an initial target of zinc oxide nanoparticles in oysters *Crassostrea gigas*, leading to mitochondrial disruption and oxidative stress. Aqua. Toxicol. 153: 27–38.

Uner, N., Oruc, E.O., Canli, M., Sevgiler, Y.,;1; 2001. Effects of cypermethrin on anti-oxidant enzyme activities and lipid peroxidation in liver and kidney of the freshwater fish, *Oreochromis niloticus* and *Cyprinus carpio* (L.). Bull.Environ. Contam. Toxicol. 67,657–664.

Vale, G., Mehennaoui, K., Cambier, S., Libralato, G., Jomini, S., Domingos, R.F.,;1; 2016. Manufactured nanoparticles in the aquatic environment-biochemical responses on freshwater organisms: A critical overview. Aqua. Toxicol. 170: 162–174.

Wolff, S.P.,;1; 1994. Ferrous ion oxidation in presence of ferric ion indicator xylenol orange for measurement of hydroperoxides. Methods Enzymol. 233,182–189.

Xu, J., Li, M., Mak, N.K., Chen, F., Jiang, Y.,;1; 2011. Triphenyltin induced growth inhibition and antioxidative responses in the green microalga *Scenedesmus quadricauda*. Ecotoxicology 20, 73–80.

Yu, T., Zeng, J., Lim, B., Xia, Y.,;1; 2010. Aqueous-phase synthesis of Pt/CeO2 hybrid nanostructures and their catalytic properties. Adv. Mater. 22, 5188-5192.

Zaroogian, G.E., Yevich, P.P.;1; 1993. Cytology and biochemistry of brown cells in *Crassostrea virginica* collected at clean and contaminate stations. Environ. Pollut. 79, 191-197.

Zhang, J., Tang, Y., Lee, K., Ouyang, M.,;1; 2010. Tailoring light–matter–spin interactions in colloidal hetero-nanostructures. Nature 466, 91-95.

</BIBL>

Table and figures legends:

<Figure>**Figure 1.** XRD patterns of pure ZnO NPs and ZnO-decorated AuNPs.

<Figure>**Figure 2.** TEM images (a,b), EDX spectrum (c) and selected area electron diffraction (SAED) pattern (d) of the ZnO-decorated AuNPs.

<Figure>**Figure 3:** Dynamic light scattering (DLS) of Au-ZnO nanoparticles dispersed in seawater

<Figure>**Figure 4:** Free iron (a), Ionizable calcium (b), Superoxide dismutase activity (c), hydrogen peroxide level (d), Catalase activity (e) and Malondialdehyde (f) in the gill and digestive gland of Control and treated clams with Au-ZnONP50 = 50 µg/L and Au-ZnONP100 = 100 µg/L for 14 days. All values are given as means (n = 5). *, $ are significantly different at $p < 0.05$ (ANOVA, post-hoc, Tukey HSD test, STATISTICA s 8.0).

<Figure>**Figure 5:** Digestive gland of control clams after 0 and 14 days (A and B), exposed clams to Au-ZnONP50 = 50 µg/L (C) and exposed clams to Au-ZnONP100 = 100 µg/L for 14 days (D) stained with hematoxylin/eosin. Exposed clams to Au-ZnONP100 showed atrophy of digestive tubules (1), diffuse hemocytic infiltration (2), Brown cells (3) and Vacuolation (4) in the digestive tubule (DT). Scale bars: 1mm

<Figure>**Figure 6:** Histopathological conditions. (A and B): Gill of control clam after 0 and 14 days; (C): Gills of exposed clams to Au-ZnONP50 = 50 µg/L; (D) Gills of exposed clams to Au-ZnONP100 = 100 µg/L for 14 days stained with hematoxylin/eosin. Exposed clams to Au-ZnONP100 showed Vacuolation (1) of gill filaments and Brown cells (2). Scale bars: 1 mm

<Table>Table 1**:** Heavy metal content in the whole soft tissue (mg kg^{-1} dry weight; mean ± SD, n = 5) of Control and treated clams with Au-ZnONP50 = 50 µg/L and Au-ZnONP100 = 100 µg/L

	Dry weight (g)	Au	Zn	Fe	Cu	Mn
Control clams	0.446 ± 0.025	ND	2.09 ± 0.921	0.75 ± 0.353	0.25 ± 0.031	0.355 ± 0.003
Treated clams with Au-ZnONP50	0.510 ± 0.031	6.09 ± 1.45 *	2.857 ± 0.208	1.075 ± 0.176	0.287 ± 0.024	0.365 ± 0.025
Treated clams with Au-ZnONP100	0.337 ± 0.018	46.97 ± 5.17*	15.248 ± 0.025*	2.125 ±1.84*	0.451 ± 0.026*	0.387 ± 0.027

ND: Not detected

*: significant difference from control at $p < 0.05$

TDENDOFDOCTD